^{133}Cesium HYSCORE Investigation of the Di-*tert*-butyl Nitroxide−Cs^+ Adsorption Complex in CsNaY Zeolite

Marlen Gutjahr,* Rolf Böttcher, and Andreas Pöppl

Faculty for Physics and Earth Science, Institute for Experimentally Physics II, University of Leipzig, Linnéstr. 5, D-04103 Leipzig, Germany

Received: May 29, 2003; In Final Form: September 10, 2003

^{133}Cs hyperfine sublevel correlation (HYSCORE) spectroscopy has been employed to characterize the structure of adsorption complexes of di-*tert*-butyl nitroxide (DTBN) with cesium cations in zeolite CsNaY. The experimental ^{133}Cs HYSCORE data proved the direct coordination of the adsorbed DTBN molecules to the Cs^+ ions and revealed nonambiguously the existence of two different types of adsorption complexes. Evaluation of the orientation selective ^{133}Cs HYSCORE spectra provided the ^{133}Cs hyperfine coupling tensors and thus information about the geometrical structure of those complexes. For one type of adsorption complexes, a complex geometry was obtained where the Cs^+ ion is located within the molecular mirror plane of the DTBN radical with an oxygen−cesium cation bond length of 0.25 nm. For this, the isotropic Cs hyperfine coupling was negative. The second Cs^+−DTBN complex is characterized by a bent structure. With an isotropic ^{133}Cs hyperfine coupling of 9 MHz, the unpaired electron spin density in this Cs^+−DTBN complex localized at the Cs ion was 0.36%.

1. Introduction

Crystalline alumosilicates known as zeolites are used in a wide area of application as, for example, in the field of adsorption and catalysis.[1] Because of the huge inner surface of these materials, their form selectivity, and the possible existence of acidic sites, zeolites are employed as catalysts in the field of heterogeneous catalysis. Acidic adsorption sites in zeolites are Broenstedt acid sites (proton donors), which are assigned to OH groups within the zeolite and Lewis acid sites (electron pair acceptors). Adsorption sites in zeolites showing Lewis acidity can either be aluminum defect centers or alkali metal cations. To characterize adsorption sites in zeolites, one promising approach is the complexation with paramagnetic probe molecules such as nitroxide radicals and the subsequent investigation of the formed adsorption complexes by means of electron spin resonance (ESR) spectroscopy. ESR investigations can provide information about the electron pair acceptor properties of the adsorption sites since the nitrogen hyperfine (hf) coupling is a direct and sensitive measure. Recently, continuous wave (cw) ESR studies proved the Lewis acidic properties of alkali metal ions in zeolite Y by using the di-*tert*-butyl nitroxide (DTBN) as probe molecule.[2] Generally, five charge-balancing cation sites SI, SI′, SII, SII′, and SIII are known for the faujasite type Y zeolite[3] (Figure 1). Because of the size of the DTBN molecules,[4] the probe molecules can only form adsorption complexes with cation sites within the supercage of the faujasite framework. To gain insight about the symmetry and structure of the adsorption complexes formed by the nitroxide radical and the zeolite cations, information is required about the alkali metal ion hf coupling. Since the spectral resolution of cw ESR experiments is not sufficient to resolve the cesium hf coupling, high-resolution pulsed ESR methods have to be applied.

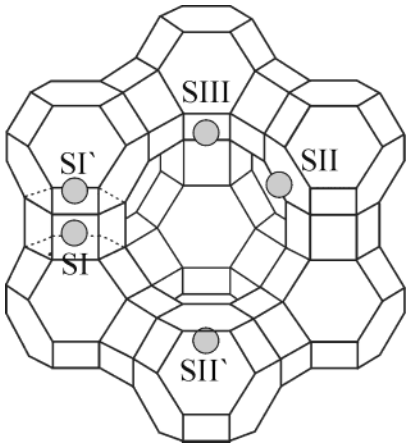

Figure 1. Schematic representation of faujasite type zeolite indicating the cationic sites SI, SI′, SII, SII′, and SIII.

Electron nuclear double resonance (ENDOR) and one-dimensional (1D) electron spin−echo envelope modulation (ESEEM) spectroscopy are well-established techniques for the measurement of weak hf and nuclear quadrupole (nq) interactions. However, the interpretation of ENDOR and 1D ESEEM spectra of disordered systems such as zeolites is often complicated because of broad overlapping signals in spectra of disordered systems. Two-dimensional (2D) ESEEM sequences such as the four-pulse or hyperfine sublevel correlation (HYSCORE) spectroscopy have been developed to overcome this problem.[5] The HYSCORE experiment with the pulse sequence ($\pi/2-\tau-\pi/2-t_1-\pi-t_2-\pi/2-\tau-$echo) is based on the creation of correlations between nuclear coherences of two different electron spin manifolds with the nuclear transition frequencies ω_{ij} and ω_{lm}. These correlations lead to cross-peaks at (ω_{ij}, ω_{lm}), (ω_{lm}, ω_{ij}), and ($-\omega_{ij}$, ω_{lm}), ($-\omega_{lm}$, ω_{ij}) in the 2D Fourier transformed (FT) HYSCORE spectra depending on the mag-

* Address correspondence to this author. Phone: 0341/9732610; fax: 0341/9732649; e-mail: marlen@physik.uni-leipzig.de.

10.1021/jp030672m CCC: $25.00 © 2003 American Chemical Society
Published on Web 11/05/2003

nitude of the hf and the nq interaction with respect to the nuclear Larmor frequency. The spread into two dimensions improves significantly the spectral resolution of the ESEEM spectra. By analyzing the shape and the position of the correlation features, the hf and nq parameters can be determined. In most of the experimental cases, especially in disordered systems, the 2D approach provides more information than the 1D techniques.

Recently, we have presented a Li HYSCORE study for the structural characterization of a DTBN:Li^+ adsorption complex formed in a lithium-exchanged Y zeolite by 2D ESEEM spectroscopy.[6] It was not only possible to prove the direct coordination of the adsorbate nitroxide radicals to the Li^+ cations but also to determine the NO−Li bond length and the geometrical structure of the DTBN:Li^+ adsorption complex. Only a few applications of the HYSCORE experiment for nuclei with nuclear spin $I = 3/2$ such as the ^{7}Li isotope or $I = 5/2$ like ^{25}Al are known,[7−9] but to our knowledge this method has not been utilized for the investigation of $I = 7/2$ nuclei such as ^{133}Cs. Therefore, before discussing the experimental ^{133}Cs HYSCORE data, the characteristics of such spectra as well as the influence of the hf interaction on the cross-peak ridges are discussed. To study the coordination geometry of DTBN, adsorption complexes formed with Cs^+ cations in zeolite CsNaY orientation selective ^{133}Cs HYSCORE experiments were carried out.

2. Experimental Section

The faujasite type zeolite CsNaY was prepared by ion exchange with cesium chloride from a NaY with a Si/Al ratio of 2.5 provided by UOP (LOT/5237-35). The ion exchange was carried out under stirring of 1 g NaY zeolite with a 0.1 M cesium chloride solution at 353 K for 12 h. This procedure was repeated three times and the CsNaY thus obtained was dried overnight at 373 K. In this way, a cesium exchange rate of about 70% could be attained. For the further sample preparation, 30 mg of zeolite was placed in a 3-mm quartz glass tube and heated under vacuum from room temperature to the activation temperature of 670 K over a period of 48 h. The activation temperature was held for at least 2 h and the final vacuum was 0.01 Pa. The adsorbate vapor was transferred to the zeolite sample by immersing the latter in liquid nitrogen.

The 2D ESEEM experiments were carried out at 15 K using a Bruker ESP 380 FT ESR spectrometer working at X band frequencies. For the HYSCORE experiments, mw pulse lengths of $t_{\pi/2} = 16$ ns for $\pi/2$ pulses and $t_\pi = 32$ ns for π pulses were applied. The orientation selective HYSCORE measurements were done at various spectral positions within the DTBN ESR spectrum. To minimize the problem of the blind spot effect, the experiments were employed with different pulse delays τ. A 170 × 170 2D data matrix was sampled with dwell times of 32 ns. Baseline correction was done by subtracting a third-order polynomial of the experimental data set in both time domains. 2D FT magnitude spectra were calculated and presented as contour plots.

The simulations of the HYSCORE spectra were calculated in the time domain by exact diagonalization of the spin Hamiltonian. Ideal nonselective microwave (mw) pulses were used, a finite excitation range of the mw pulses was taken into account in the calculation of the orientation selective ESEEM spectra by assuming an inhomogeneous line broadening of the ESR signal of 0.6 mT. Subsequently, the time domain spectra were zero filled and transformed into the frequency domain by Fast Fourier Transformation. For further information concerning the procedure for the calculation of the four-pulse ESEEM modulation, we refer to an earlier paper.[10]

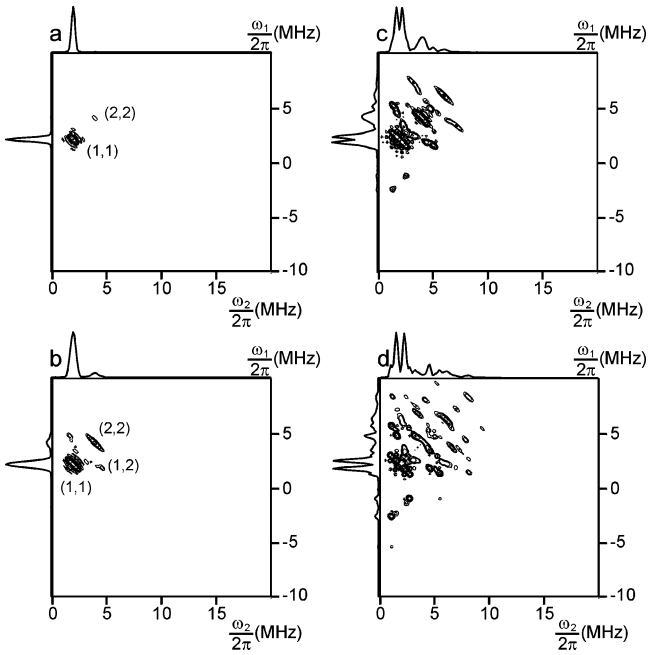

Figure 2. Simulated powder HYSCORE spectra for an $S = 1/2$, $I = 7/2$ spin system showing the effect of the $T_\perp$ magnitude. Simulation parameters are $\omega_I/2\pi = 1.94$ MHz, $A_{iso} = 0$, $Q_{zz} = 0$, $T_\perp = 0.3$ MHz (a), $T_\perp = 0.5$ MHz (b), $T_\perp = 0.7$ MHz (c), and $T_\perp = 0.9$ MHz (d).

3. Results

3.1. General Interpretation of $I = 7/2$ HYSCORE Spectra. ^{133}Cs is a nucleus with nuclear spin $I = 7/2$, which means that the two electron spin manifolds α (belonging to the electron spin quantum number $M_S = 1/2$) and β ($M_S = -1/2$) split into eight levels according to the nuclear spin quantum numbers $M_I = (7/2, 5/2, \ldots -5/2, -7/2)$. Because of the nq interaction, the energy levels are no longer equidistant but shifted proportionally to M_I^2. Consequently, the HYSCORE spectrum of a spin system with electron spin $S = 1/2$ and nuclear spin $I = 7/2$ consists theoretically of $2(2I)^2 = 98$ correlation peaks from exclusively $|\Delta M_I| = 1$ nuclear transitions in the following labeled with (1,1) and a variety of correlation peaks with $|\Delta M_I| = 2$ or $|\Delta M_I| = 3$ transitions. Fortunately, the intensity of most of the correlation peaks is very low, so that the majority of the cross-peaks is not detectable. For that reason, the resolution enhancement of the HYSCORE experiment with respect to 1D approaches because of the spread into two dimensions is also valid for spin systems with $I > 1$.

Since the HYSCORE experiment was not applied to nuclei with $I = 7/2$ so far, we will first discuss the characteristics of $S = 1/2$, $I = 7/2$ HYSCORE spectra with an isotropic electron **g** tensor in dependence of the isotropic and the dipolar part A_{iso} and $T_\perp$, respectively, of the hf coupling of the $I = 7/2$ nucleus. By means of simulated HYSCORE data of a ^{133}Cs nucleus with $\omega_I/2\pi = 1.94$ MHz, the influence of the magnitude of the ^{133}Cs hf interaction on line shape and position of the cross-peak ridges is shown. To concentrate on the specific influence of the Cs hf coupling, the nq coupling was set to zero for the calculations. The latter is reasonable since the electric quadrupole moment of ^{133}Cs is very small compared to the majority of other nuclei having $I > 1/2$ that are of interest for ESEEM experiments. Therefore, the number of $|\Delta M_I| = 1$ transition peaks in one quadrant is reduced to two cross-peaks.

Figure 2 presents four calculated HYSCORE powder spectra with different values for $T_\perp$. First of all, the increasing number of cross-peak ridges with rising $T_\perp$ is striking. Signals belonging

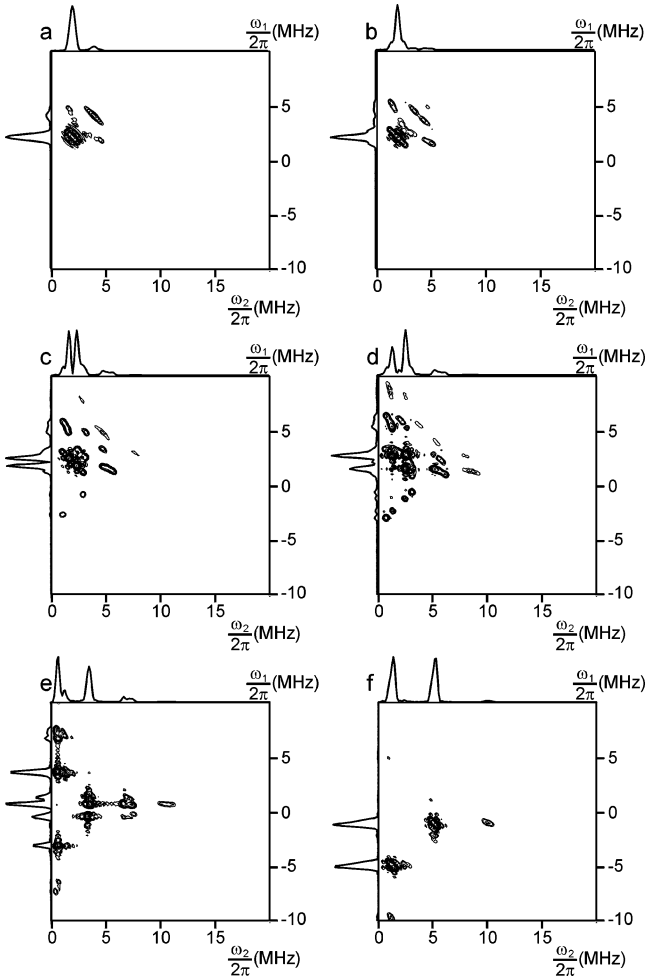

Figure 3. Simulated powder HYSCORE spectra for an $S = 1/2$, $I = 7/2$ spin system showing the effect of the A_{iso} magnitude. Simulation parameters are $\omega_I/2\pi = 1.94$ MHz, $T_\perp = 0.5$ MHz, $Q_{zz} = 0$, $A_{iso} = -0.5$ MHz (a), $A_{iso} = 0.5$ MHz (b), $A_{iso} = 1.0$ MHz (c), $A_{iso} = 1.5$ MHz (d), $A_{iso} = 3.0$ MHz (e), and $A_{iso} = 6.0$ MHz (f).

to $|\Delta M_I| = 2$ transitions appear with sufficient intensity in the 2D spectrum not until $T_\perp \geq 0.3$ MHz and cross-peaks with $|\Delta M_I| > 2$ are only noticed for $T_\perp \geq 0.5$ MHz. Generally, the larger the appropriate $|\Delta M_I|$ values are, the lower the intensity of the correlation peaks in a HYSCORE spectrum is. Concordant for the 1D two-pulse and three-pulse ESEEM experiment, a strong decrease of the echo modulation amplitude with increasing $|\Delta M_I|$ was found.[11]

As shown for spin systems with $S = 1/2$, $I = 3/2$, it is possible to estimate the magnitude of $T_\perp$ from the maximum vertical shift of the (1,1) and (2,2) ridges (naming ridges belonging to ($|\Delta M_I| = 1$, $|\Delta M_I| = 1$) and ($|\Delta M_I| = 2$, $|\Delta M_I| = 2$) transitions) to higher frequencies with respect to the $\omega_1 = -\omega_2$ axis.[12] This approach was deduced for $S = 1/2$, $I = 1/2$ systems[13] but is also applicable for systems with $I > 1/2$. A comparison between $T_\perp$ values used for the simulated ^{133}Cs spectra and those that were determined from the shift of the (1,1) and (2,2) ridges result in a good agreement, particularly for $T_\perp \geq 0.3$ MHz. In analogy to the results for spin systems with $I = 3/2$ nuclei, the accuracy is much better by means of the so-called double quantum peaks (2,2).

Second, the influence of the isotropic part of the hf on the HYSCORE powder pattern was studied. For this purpose, spectra were calculated with $T_\perp = 0.5$ MHz and varying values for A_{iso} (Figure 3). With growing A_{iso} the total extent of the spectrum is increasing. Signals within the second quadrant of

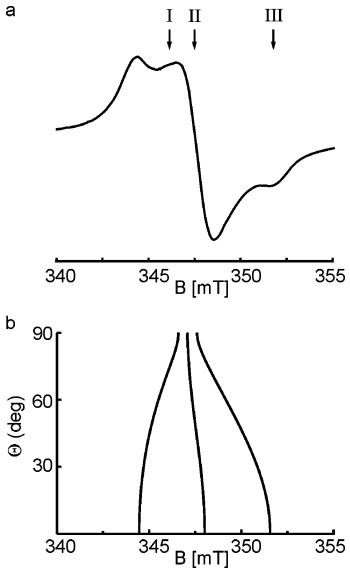

Figure 4. (a) ESR spectrum of the DTBN:Cs^+ adsorption complex at 20 K. The arrows indicate the spectral positions I, II, and III, where orientation selective HYSCORE measurements were done. (b) Calculated ^{14}N resonance fields in dependence on the angle Θ between the g_{zz} axis and the external magnetic field.

the HYSCORE spectrum occur for the first time with $A_{iso} = 1.0$ MHz. These signals become more intense with larger A_{iso} whereas simultaneously the cross-peaks within the first quadrant loose intensity. Thus, the spectrum with $A_{iso} = 6$ MHz contains only cross-peak ridges at negative ω_1 values in the second quadrant. This behavior is likewise well known for $S = 1/2$, $I = 1/2$ systems; for this purpose, analytical expressions were derived by Gemperle et al.[14]

3.2. HYSCORE of Cs^+−DTBN Complexes in CsNaY. Recently, ESR measurements of DTBN adsorbed on several alkali metal ion exchanged Y zeolites demonstrated the Lewis acidic properties of the alkali metal ions.[2] It was shown that the ^{14}N hf coupling is a sensitive measure for the electron pair acceptor properties of the adsorption sites. Moreover, the ESR results suggested the direct coordination of the DTBN molecules to the alkali ions within the zeolite at low temperatures. To confirm the formation of adsorption complexes with the metal ions in cesium exchanged Y zeolite, ^{133}Cs 2D HYSCORE experiments were performed. In Figure 4a, an experimental ESR spectrum of DTBN sorbed on the cesium form of zeolite Y at 20 K is presented showing the different field positions for the HYSCORE experiments. Figure 4b displays the calculated ESR resonance positions in dependence on the angle Θ between the external magnetic field **B** and the $g_\parallel$ axis of the DTBN **g** tensor. The presented angular dependence was calculated with the spin-Hamiltonian parameters known from the simulation of the experimental ESR powder spectrum.[2] It is characterized by an axially symmetric electron Zeeman tensor **g** with $g_\parallel = 2.0023$, $g_\perp = 2.0075$, and a coaxial ^{14}N hf interaction tensor $\mathbf{A^N}$ with $A_\parallel = 3.55$ mT, $A_\perp = 0.5$ mT.

^{133}Cs HYSCORE experiments were done at three different field positions within the ESR powder pattern that are indicated by arrows within Figure 4a. The orientations with $\Theta = 90°$ and $\Theta = 0$ correspond to the $g_\perp$ (I) and $g_\parallel$ (III) position in Figure 4, whereas at the spectral position II, the so-called powder position, crystallites with **g** tensors contribute to the ESR powder pattern whose angle Θ is in the range of $0° \leq \Theta \leq 90°$. Figure 5 displays experimental ^{133}Cs HYSCORE spectra at these three field positions and appropriate simulations. All spectra show ridges at (∼15 MHz, ∼15 MHz) belonging to the protons of

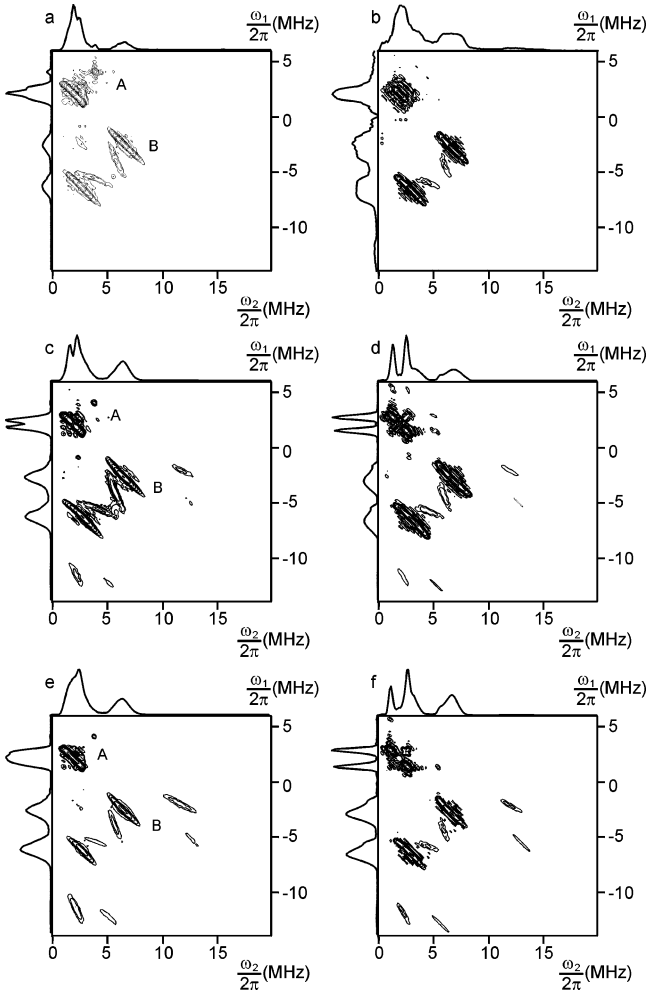

Figure 5. Experimental (a, c, e) and simulated (b, d, f) ^{133}Cs HYSCORE spectra of the DTBN−Cs^+ adsorption complexes at the spectral position I (a, b), II (c, d), and III (e, f) with $\tau = 96$ ns.

the CH_3 groups of the DTBN molecules. Because these spectral features are of no interest for the structural characterization of the Cs^+−DTBN complexes, the following presentations of the experimental data show only the cesium part of the HYSCORE spectra. In contrast to HYSCORE measurements of Li^+−DTBN complexes in LiY zeolites, signal intensity is not only within the first but also in the second quadrant of the HYSCORE pattern. As we have shown before, this indicates that there is a complex structure with relatively large isotropic Cs hf coupling ($|A^{Cs}/2| > \omega_I{}^{Cs}/2\pi$). Since the experimental spectra also show cross-peaks in the (+,+) quadrant attributed to a complex with $|A^{Cs}/2| < \omega_I{}^{Cs}/2\pi$, the existence of two different geometrical structures for the Cs^+−DTBN adsorption complex (labeled with A and B) seems to be supposable. The second possible explanation of one electron interacting with two cesium nuclei could be excluded since that would lead to combination peaks between the two sets of cross-peaks A and B, which were not found in the experimental data.

Moreover, the existence of two different Cs^+−DTBN adsorption complexes was confirmed by simulating the experimental Cs HYSCORE data. Only with two structural complexes, the simulations result in good concordance with the experimental HYSCORE spectra. The principal values of the ^{133}Cs hf coupling tensor were $A_{xx}^{Cs} = A_{yy}^{Cs} = \pm 1.7$ MHz and $A_{zz}^{Cs} = \pm 0.5$ MHz for adsorption complex A and $A_{xx}^{Cs} = A_{yy}^{Cs} = \pm 7.2$ MHz and $A_{zz}^{Cs} = \pm 12.6$ MHz for adsorption complex B.

By means of orientation selective measurements of the Cs^+−DTBN adsorption complex in zeolite CsNaY, it was also possible to evaluate the orientation of $\mathbf{A}^{Cs}$ with respect to the **g** tensor principal axes system defined by a set of Euler angles (α, β, γ). The angle β between A_{zz}^{Cs} and g_{zz} amounts for complex A to 90° and a distribution of complex structures was found according to a distribution of the Euler angle β with $\Delta\beta = \pm 25°$. For the Cs^+−DTBN adsorption complexes of type B, which are characterized by a relatively strong Cs hf coupling, the angle between the axes A_{zz}^{Cs} and g_{zz} is $\beta = (50° \pm 25°)$. Because of the axial symmetry of both the **g** and $\mathbf{A}^N$ tensor, the angle α describing the NO−Cs^+ bond within the (g_{xx}−g_{yy}) plane could not be determined.

Since the experimental cesium cross-peaks do not show any nq splitting, it was not possible to obtain the exact values for the principal values $Q_{xx} = Q_{yy}$ and $Q_{zz} = -Q_{xx}/2$ of the nq coupling tensor **Q**. By evaluating the ^{133}Cs HYSCORE spectra, an upper limit for Q_{zz} was 0.01 MHz.

4. Discussion

The Cs HYSCORE spectra revealed two kinds of Cs^+−DTBN adsorption complexes with different complex geometries. For complex structure A, a great similarity to the Li^+−DTBN complex in zeolite LiY was found. From the principal values of that Cs^+−DTBN complex A, we determine an isotropic hf coupling $A_{iso}^{Cs} = -1.3$ MHz. To simulate the large intensity in the middle of the (1,1) ridges in the experimental data, a distribution of $A_{iso}^{Cs} = (-1.3 \pm 0.3)$ MHz was assumed. The negative spin density in the Cs 6s orbital is due to spin polarization effects. A similar finding was made for Li^+−DTBN adsorption complexes in zeolite LiY for which a negative isotropic metal ion hf coupling was revealed, too.[6] Furthermore, Chuvylkin et al. did quantum chemical calculations regarding the coordination of nitroxide probes to Al^{3+} ions acting as Lewis acid sites on the surface of Al_2O_3.[15] Al^{3+} ions have an equal number of outer-shell electrons such as the Li^+ and Cs^+ ions so that a comparison of our experimental results with those calculations will be appropriate. In case of coordination to the aluminum via the oxygen of the NO group, these calculations result in negative values for A_{iso}^{Al} in good agreement with our experimental findings.

The structure of both the Cs^+−DTBN complexes A and B can be deduced from the principal values of their Cs hf tensor and its orientation with respect to the coordinate frame of the **g** and $\mathbf{A}^N$ tensors. From $\mathbf{A}^{Cs}$ and A_{iso}^{Cs}, the principal values of the cesium dipolar hf coupling tensor $\mathbf{T}^{Cs}$ were $T_{xx}^{Cs} = T_{yy}^{Cs} = -0.4$ MHz and $T_{zz}^{Cs} = 0.8$ MHz for complex A and $T_{xx}^{Cs} = T_{yy}^{Cs} = -1.8$ MHz and $T_{zz}^{Cs} = 3.6$ MHz for complex B.

Using a dipole−dipole approximation and taking into account the interactions of the ^{133}Cs nuclear spin with both the electron spin densities at nitrogen and oxygen, ρ_π^N and ρ_π^O, respectively, we can construct $\mathbf{T}^{Cs}$ by two tensor contributions $\mathbf{T}_{O-Cs}^{Cs}$ and $\mathbf{T}_{N-Cs}^{Cs}$, which can be calculated in the **g** tensor frame according to Hutchinson and McCay.[16] Knowing the N−O bond distance of the DTBN molecule $r_{N-O} = 0.128$ nm[4] and the unpaired π electron spin density at the nitrogen atom $\rho_\pi^N = 60\%$ from earlier ESR investigations,[2] the dipolar coupling tensor $\mathbf{T}^{Cs}$ is the sum of the two tensors $\mathbf{T}_{O-Cs}^{Cs}$ and $\mathbf{T}_{N-Cs}^{Cs}$

$$\tilde{\mathbf{R}}(\alpha,\beta,\gamma)\mathbf{T}^{Cs}\mathbf{R}(\alpha,\beta,\gamma) = \mathbf{T}_{O-Cs}^{Cs}(\rho_\pi^O, r_{O-Cs}, \beta_{bond}) + \mathbf{T}_{N-Cs}^{Cs}(\rho_\pi^N, r_{N-Cs}, \beta_{bond}) \quad (1)$$

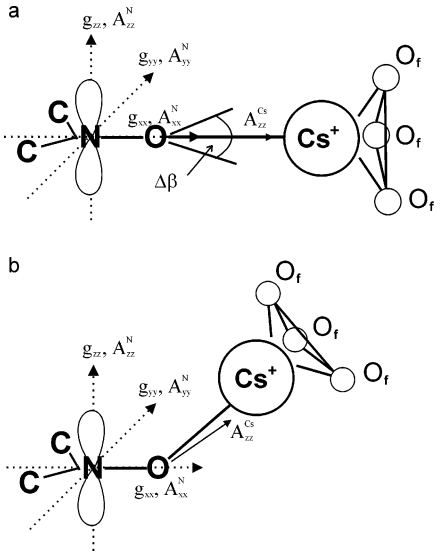

Figure 6. Structural models of the DTBN−Cs^+ adsorption complexes zeolite CsNaY (with the framework oxygen of the zeolite indicated by O_f): (a) complex geometry A with a bond length $R_{O-Cs} = 0.25$ nm and $\beta_{bond} = 180° \pm 25°$; (b) complex structure B with $R_{O-Cs} = 0.21$ nm and $\beta_{bond} = 137° \pm 25°$.

The Euler matrix **R** transforms the diagonal tensor $\mathbf{T}^{Cs}$ in the **g** tensor frame. The bond angle is defined by $\beta_{bond} = 180° - \alpha_O$ with α_O naming the angle between the vector $\vec{r}_{O-Cs}$ pointing from the oxygen atom of DTBN to the Cs cation and the g_{zz} direction.

In complex A with an angle between the *z*-axes of the **g** and $\mathbf{T}^{Cs}$ tensors of $\beta = 90°$ and T^{Cs}_{zz} is within the **g** tensor *xy*-plane (Figure 6a), the solution of eq 1 is more straightforward. Under the assumption that the sum of ρ^N_π and the unpaired π electron spin density at the oxygen atom ρ^O_π is $\rho^N_\pi + \rho^O_\pi = 1$, we deduce from the obtained Cs dipolar hf coupling constant $T_\perp{}^{Cs} = 0.4$ MHz the distance between the Cs^+ cation and the oxygen atom of the NO group $R_{O-Cs} = 0.25$ nm. This result proves the direct coordination of the probe molecules to the cesium cations; the larger bond length of the cesium adsorption complex A compared with that of the lithium complex in LiY $r_{O-Li} = 0.19$ nm is mainly due to the differences in the ionic radius, that is, 0.06 nm for lithium and 0.169 nm in cesium.[17] Comprehensively, the orientation selective Cs HYSCORE measurements provide a structural model for the Cs^+−DTBN complex A that has a linear but distributed structure according to $\beta = 90° \pm 25°$ (Figure 6a).

Regarding the second complex structure B for the Cs^+−DTBN adsorption complexes, the principal values of the Cs hf coupling tensor leads to a dipolar hf $T_\perp{}^{Cs} = 1.8$ MHz. With $\beta = 50°$, it is possible to determine by a numerical solution of eq 1 $R_{O-Cs} = 0.21$ nm and $\beta_{bond} = 137°$. Here, $\rho^N_\pi + \rho^O_\pi = 1$ with $\rho^N_\pi = 60\%$ was assumed again. Considering the ionic radius of Cs^+ $R_{Cs} = 0.169$ nm, the calculated bond length of 0.21 nm seems to be quite reasonable. According to $\beta_{bond} = 137°$, the mean complex structure of adsorption complex B is no longer linear but bent; the structural model following from these calculations is shown in Figure 6b. As a result of the tilt of the mean O−Cs bond out of the *xy*-plane, an admixture of the 6s cesium orbital to the ground state of the unpaired electron located in a π orbital is supposable. The latter would lead to a nonzero contribution of spin density at the cesium ion. Indeed, a quite large positive isotropic Cs hf coupling $A^{Cs}_{iso} = 9$ MHz was found for this complex. This translates into an unpaired electron spin density in the Cs 6s orbital of $\rho^{Cs}_{6s} = 0.36\%$.

Finally, the origin of the different geometrical structures for the Cs^+−DTBN adsorption complexes has to be clarified. ESEEM studies of DTBN adsorbed at zeolite LiY showed only structure A for the Li^+−DTBN adsorption complexes.[6] As mentioned above, DTBN probe molecules can only form adsorption complexes with cations that are located on sites in the so-called supercages (SII and SIII) of the Y zeolite. It is known from neutron diffraction and XRD investigations that in the LiY zeolite only the SII site, that is situated within the supercage next to the six-ring windows of the sodalite units, but not the SIII site in front of the four-ring windows within the supercages is occupied by Li ions.[18,19] Contrary to that, studies of the cesium-exchanged Y zeolite have demonstrated that the cesium ions are located at both SII and SIII sites.[20−23] Therefore, the DTBN molecules can find two possible adsorption sites and thus form two different adsorption complexes with Cs^+ cations in NaCsY zeolites. Since it is well known that mainly supercage Na^+ ions are exchanged by cesium ions, [20,21,24] the remaining Na^+ ions are expected to occupy nonsupercage positions. Because of the size of the DTBN radicals, these cation sites are not accessible for the probe molecules so that no adsorption complexes with the Na^+ cations can be formed.

The similarity with the Li^+−DTBN complexes suggests the SII position for the Cs^+−DTBN adsorption complex A. Opposite to the SII sites within the supercages of faujasites there is the 12-ring aperture (diameter 0.74 nm) to the three-dimensional channel system. This accounts for the formation of adsorption complexes with a linear coordination geometry in the adsorption of nitroxide probe molecules at the SII sites. In contrast to that, opposite to each SIII site within the supercages there is another SIII site. The latter prevents the coordination of the DTBN molecules to the cesium cation at the SIII sites with a linear geometry. Consistently, a bent coordination structure was found for these adsorption complexes. With a bond angle of 137°, the DTBN molecules adsorbed at SIII cesium ions may also protrude into the 12-ring apertures.

The maximum stretch of the DTBN probe molecules (0.68 nm) and the aperture of the faujasite supercages (diameter of 12-ring windows is 0.74 nm) are similar in size. Considering additionally the relative large diameter of the Cs^+ ions ($\approx$0.34 nm) together with the respective R_{O-Cs}, both experimentelly found adsorptions complexes fill in the supercages (diameter $\approx$1.3 nm) of the CsNaY zeolite to a great extent. The complex B that is formed with the Cs^+ ion residing at the SIII position is forced to a bent complex structure by those geometric constrictions, as already discussed. This bent complex structure allows the adsorbed DTBN radical to protrude into the 12-ring windows just like the DTBN radicals in the linear adsorption complexes A formed with SII Cs^+ ions. Thus, for both complex structures the methyl groups of the DTBN molecules approach quite close to the zeolite wall of the respective supercage opening.

Both the Cs^+−DTBN adsorption complexes at site SII and at site SIII show a distribution of complex structures according to the experimentally found maximum tilt angle of 25°. This result matches with the confinement of the adsorbed DTBN molecules because of the zeolite lattice. Admittedly, one has to remark that the determined tilt angle is only an approximate value because for the exact calculation the individual contributions of the orbitals have to be summed.

5. Conclusions

^{133}Cs HYSCORE spectroscopy of DTBN adsorbed in cesium-exchanged Y zeolites evidences the direct coordination of the

nitroxide molecules to the metal cation and provides insight in the geometry of the formed adsorption complexes. The existence of two different complex structures is proven. Orientation selective measurements reveal the determination of the Cs hyperfine coupling tensors for both types of adsorption complexes. Subsequently, the geometrical structure of these complexes is ascertained.

One of the complex geometries is similar to that found recently for Li^+−DTBN complexes in LiY zeolites. It has a mean linear complex geometry with an oxygen−cesium bond length of 0.25 nm. It is located at the SII cation site and underlies a distribution of complex structures. The isotropic Cs hf coupling is negative and is due to spin polarization effects, since in a linear complex geometry no admixture of the metal s orbitals to the wave function of the unpaired electron is possible.

The second Cs^+−DTBN adsorption complex formed in cesium-exchanged Y zeolites is characterized by a bent complex structure. The bond angle amounts to 137°. Consistent with the bent geometry, the isotropic Cs hf coupling is relatively large; $A_{iso}^{Cs} = 9$ MHz translates into an unpaired electron spin density in the Cs 6s orbital of $\rho_{6s}^{Cs} = 0.36\%$. The location of this complex is the SIII site within the faujasite supercage. The distribution of structures for both complexes according to the experimentally found maximum tilt angle of 25° corresponds to the confinement of the DTBN molecules because of the zeolite lattice.

Finally, we have to summarize that even for nuclei with $I = 7/2$ the 2D HYSCORE technique is succeeding in the structural characterization of complexes formed by paramagnetic probe molecules with cationic adsorption sites in zeolites. This demonstrates again the great potential of this high-resolution ESEEM method with regard to the structure determination of adsorption complexes in disordered systems.

Acknowledgment. This research was supported by the Deutsche Forschungsgemeinschaft within the Sonderforschungsbereich 294 (Moleküle in Wechselwirkung mit Grenzflächen), Teilprojekt F7 and by the German Fonds der Chemischen Industrie.

References and Notes

(1) *Catalysis and Adsorption by Zeolites*; Ohlmann, G., Pfeifer, H., Fricke, R., Eds.; Elsevier: Amsterdam, 1991.

(2) Gutjahr, M.; Pöppl, A.; Böhlmann, W.; Böttcher, R. *Colloids Surf., A* **2001**, *189*, 93.

(3) Hunger, M.; Schenk, U.; Buchholz, A. *J. Phys. Chem. B* **2000**, *104*, 12230.

(4) Andersen, B.; Andersen, P. *Acta Chem. Scand*. **1966**, *20*, 2728.

(5) Höfer, P.; Grupp, A.; Nebenführ, G.; Mehring, M. *Chem. Phys. Lett.* **1986**, *132*, 279.

(6) Gutjahr, M.; Böttcher, R.; Pöppl, A. *J. Phys. Chem*. **2002**, *106*, 1345.

(7) Astrakas, L.; Kordas, G. *J. Chem. Phys.* **1999**, *110*, 6871.

(8) Doetschman, D. C.; Gilbert, D. C.; Dwyer, D. W. *Chem. Phys.* **2000**, *256*, 37.

(9) Carl, P. J.; Vaughan, D. E. W.; Goldfarb, D. *J. Phys. Chem. B* **2002**, *106*, 5428.

(10) Pöppl, A.; Hartmann, M.; Böhlmann, W.; Böttcher, R. *J. Phys. Chem. A* **1998**, *102*, 3599.

(11) Ponti, A. *J. Magn. Reson*. **1997**, *127*, 87.

(12) Gutjahr, M.; Böttcher, R.; Pöppl, A. *Appl. Magn. Reson.* **2002**, *22*, 401.

(13) Pöppl, A.; Kevan, L. *J. Phys. Chem*. **1996**, *100*, 3378.

(14) Gemperle, C.; Aeble, G.; Schweiger, A.; Ernst, R. R. *J. Magn. Reson.* **1990**, *88*, 241.

(15) Chuvylkin, N. D.; Tokmachev, A. M.; Fionov, A. V.; Lunina, E. V. *Russ. Chem. Bulletin* **1997**, *46*, 1649.

(16) Hutchinson, C. A.; McCay, D. B. *J. Chem. Phys*. **1977**, *66*, 3311.

(17) Pauling, L. *Natur der chemischen Bindung*; Verlag Chemie: Weinheim/ Bergstr., 1964; p 475.

(18) Forano, D.; Slade, R. C. T.; Krogh Andersen, E.; Krogh Andersen, I. G.; Prince, E. *J. Solid State Chem.* **1989**, *82*, 95.

(19) Herden, H.; Einicke, W.-D.; Schöllner, R.; Motier, W. J.; Gellens, L. R.; Uytterhoeven, J. B. *Zeolites* **1982**, *20*, 131.

(20) Malek, A.; Ozin, G. A.; Macdonald, P. M. *J. Phys. Chem.* **1996**, *100*, 16662.

(21) Jelinek, R.; Malek, A.; Ozin, G. A. *J. Phys. Chem.* **1995**, *99*, 9236.

(22) Godber, J.; Baker, M. D.; Ozin, G. A. *J. Phys. Chem.* **1989**, *93*, 1409.

(23) Lai, P. P.; Rees, L. V. C. *J. Chem. Soc., Faraday Trans. 1* **1976**, *72*, 1809.

(24) Sánchez-Sánchez, M.; Blasco, T. *J. Am. Chem. Soc*. **2002**, *124*, 3443.